

Loss rate of ultracold neutrons due to the absorption by trap walls in large material traps

Pavel D. Grigoriev,^{1,2,3,*} Vladislav D. Kochev,^{2,4,1} Victor A. Tsyplukhin,² Alexander M. Dyugaev,¹ and Ilya Ya. Polishchuk^{4,5}

¹*L. D. Landau Institute for Theoretical Physics, 142432, Chernogolovka, Russia*

²*Theoretical Physics and Quantum Technologies Department,*

National University of Science and Technology "MISIS", 119049, Moscow, Russia

³*National Research University Higher School of Economics, Moscow, 101000, Russia*

⁴*NRC Kurchatov Institute, 123182, Moscow, Russia*

⁵*Theoretical Physics Department, Moscow Institute For Physics and Technology, 141700, Dolgoprudnii, Russia*

(Dated: July 4, 2024)

The most accurate neutron lifetime measurements now use the material or magnetic traps of ultracold neutrons (UCN). The precision of these experiments is determined by the accuracy of estimating the neutron loss rate. In material UCN traps the main source of neutron losses is the absorption by trap walls. In this paper we analyze the standard methods and their approximations for the calculation of UCN absorption rate by the walls of material traps. We emphasize the approximations used both in the standard analytical formulas and in the numerical Monte-Carlo simulations. For the two simplest trap geometries, rectangular and cylindrical, we obtain precise analytical formulas for this absorption rate and compare them with the standard estimation methods. The difference turned out to be considerable and especially important for the size extrapolation procedure, always used in the standard estimates of UCN losses. Our results may partially resolve the puzzling four-second discrepancy between the magnetic and material-trap measurements of neutron lifetime.

I. INTRODUCTION

The neutron β -decay $n \rightarrow p + e^- + \bar{\nu}_e$ plays an important role in cosmology, astrophysics and elementary particle physics (see [1–7] for reviews). The primordial light element abundance is very sensitive to the exact value of neutron mean lifetime τ_n [1, 8]. The precise τ_n -measurements, combined with decay correlations in polarized-neutron decay experiments [9–12], test the standard model and give the coupling constants of the weak interaction [1–4, 9–13]. The measurements of neutron electric dipole moment (EDM) [14–17] impose the upper limits on CP violation. The resonant transitions between discrete quantum energy levels of neutrons in the earth gravitational field [18–20] probe the gravitational field on a micron length scale and impose constraints on dark matter.

These and other neutron experiments mostly employ the ultracold neutrons (UCN) with energy E lower than either the neutron optical potential of typical materials or the Zeeman energy of neutron spin in available magnetic fields, i.e. $E \lesssim 300$ neV [11, 12, 14–36]. In material traps UCN can be trapped for many minutes in specially designed "neutron bottles" [24–30], where the earth gravitational field 100 neV per meter plays an important role in UCN storage and manipulation [21–28]. The Fomblin grease is currently used to cover the UCN trap walls [24–30] in the bottle UCN experiments and allows reaching the very high accuracy of neutron lifetime measurements in large gravitational traps [27]: $\tau_n = 881.5 \pm 0.7$ (stat) ± 0.6 (syst) s. The neutron magnetic moment of 60 neV/T allows magneto-gravitational trapping of UCN [31–36], giving even higher claimed accuracy of latest UCN- τ measurements [36]: $\tau_n \approx 877.7 \pm 0.28$ (stat) $^{+0.22}_{-0.16}$ (syst) s. The neutron lifetime measured using magnetic traps [36] is about 4 seconds smaller than in the UCN material-bottle experiments [27], which is beyond the 3σ deviation.

The most precise time-of-flight τ_n -measurements with the beam of cold neutrons give $\tau_n = 887.7 \pm 1.2$ (stat) ± 1.9 (syst) s [37–39], which is about 10 seconds greater than in the UCN magnetic traps. The large discrepancy between τ_n measured using the beam and UCN material- or magnetic-trap methods is called the "neutron lifetime puzzle" and receives extensive discussion till now [39–43]. Presumably, this is due to systematic errors in beam experiments [41], but unaccounted UCN losses in the bottle material and magnetic trap τ_n measurements have not yet been excluded. The analysis of neutron β -decay asymmetry [44] suggests that this discrepancy is unlikely caused by new physics, for example, by dark matter and additional neutron decay channels or excited states [39, 40].

The precision of τ_n measurements using UCN traps, both material and magnetic, is determined by the accuracy of estimating the neutron loss rate from the traps, which is the main source of systematic errors [21–28, 34–36, 45]. The main UCN loss mechanism from magnetic traps, as listed in Table II of Ref. [36], include (i) UCN spin depolarization, for example, because of the nonuniform magnetic field and, hence, its nonzero perpendicular-to-spin component; (ii) heated UCNs; (iii) residual gas scattering; (iv) uncleaned higher-energy UCNs. In this paper we do not discuss the accuracy of magnetic-trap UCN experiments and consider only the material traps.

The material UCN traps are, usually, coated with Fomblin grease, providing the highest accuracy of τ_n measurements. The Fomblin grease has the optical potential barrier $V_0^F \approx 106$ neV. The probability of neutron absorption by such a wall is $\sim 10^{-5}$ per collision [6, 21–23]. In addition, the inelastic UCN scattering by trap walls, when the neutron absorbs a thermal excitation, increases the UCN energy above the potential barrier V_0 and also leads to neutron losses. Therefore, the neutron lifetime τ_n is estimated by the double extrapolation of the measured lifetime $\tau_m < \tau_n$ of UCN stored in the trap to zero temperature (thermal extrapolation) and to an infinite trap size (geometrical or size extrapolation). The extrapolation

* Corresponding author, e-mail: grigorev@itp.ac.ru

interval is rather large, usually, $\tau_n - \tau_m \gtrsim 20$ s. This limits the precision of τ_n measurements in material traps, because the estimate of UCN loss rate with an accuracy better than 5% is very complicated.

The UCN absorption probability depends on the angle of incidence during each collision. The usually applied assumption [27] of the uniform distribution of neutron velocity direction with respect to the trap surface is violated for the collisions with side walls because the vertical UCN velocity component depends on the height above trap bottom due to gravity. This difficulty can be overcome by Monte-Carlo simulations [46–51] of UCN losses taking into account the calculated incidence angles of each collision for the particular trap geometry, provided the initial momentum distribution of UCN is known and the applied simple physical model of UCN interaction with trap walls is correct. The Monte-Carlo simulations are also actively used to estimate the UCN losses in magnetic traps [52]. A more serious problem is the surface roughness of material traps, which makes impossible the exact calculation of UCN scattering angle and loss probability during each collision.

The UCN losses on trap walls and the extrapolation interval can be reduced by increasing the trap size and, hence, the volume-to-surface ratio in material traps. However, even with a very large UCN trap with size 2 m in the recent τ_n measurements [27] the extrapolation interval $\tau_n - \tau_m$ was only reduced to 20 seconds. A further size increase of UCN traps is not only technically problematic but also not very useful, because the main UCN losses already come from their collisions with the trap bottom, and the rate of these collisions is determined by the Earth gravity and by the UCN kinetic energy $E_k < V_0$, rather than by the trap size.

A possible qualitative way to reduce the UCN absorption rate is to cover the trap walls by liquid ^4He , the only material that does not absorb neutrons [53–59]. However, covering the UCN trap walls by liquid helium has several drawbacks. First, ^4He creates a very small optical potential barrier $V_0^{\text{He}} = 18.5$ neV for neutrons, which is 5.7 times smaller than the barrier height $V_0^{\text{F}} \approx 106$ neV of Fomblin oil. Hence, the UCN phase volume and their density in such a trap is reduced by the factor $(V_0^{\text{F}}/V_0^{\text{He}})^{3/2} \approx 13.7$ as compared to the Fomblin coating, which enhances the statistical errors. The UCN production technology develops [7, 60, 61], and this reduction of neutron density may become less important than the advantage of decreasing the UCN absorption rate. The second problem with the liquid ^4He coating of UCN trap walls is that a very low temperature $T < 0.5$ K is required. At higher T the concentration of ^4He vapor is rather high, leading to the inelastic UCN scattering with large energy transfer $\sim k_B T \gg V_0^{\text{He}}$ from the vapor atoms to neutrons. The third problem with liquid ^4He is another source of inelastic UCN scattering – the thermally activated quanta of surface waves, called riplons. They lead to a linear temperature dependence of scattering rate [56], surviving even at ultra-low temperature. The strength of neutron-riplon interaction is rather small [56], which makes feasible the UCN storage in He-covered traps, and the linear temperature dependence of UCN losses due to their scattering by riplons is very convenient for taking into account this systematic error. However, the UCN scattering by riplons

strongly limits the possible advantage of using liquid helium in the UCN storage. Hence, below we consider more traditional and currently used UCN traps, where the wall material absorbs neutrons.

The "neutron lifetime puzzle", i.e. the difference between τ_n -measurements using cold neutron beam and material UCN traps, is generally attributed to the errors in beam experiments [41]. However, the 4-second discrepancy between the results of latest magnetic-trap and material-bottle τ_n measurements remains puzzling. Notably, the former also very precise measurements of UCN lifetime using a material trap gave the value [24] $\tau_n = 878.5 \pm 0.7$ (stat) ± 0.3 (sys) s, which is 3 seconds smaller than the result of Ref. [27] and much closer to the magnetic-trap τ_n measurements. The difference between Refs. [27] and [24] is not only a larger size but also the different shape of UCN trap used in the experiment [27]. As we show below, the size extrapolation used to estimate the UCN loss rate τ_{loss}^{-1} due to the absorption by trap walls is rather sensitive to the trap shape, which may easily give the 3-second difference in the measured τ_n . In this paper we reanalyze the estimate method of UCN loss rate τ_{loss}^{-1} from the absorption by trap walls and indicate several important assumptions which may lead to errors in the extracted value of neutron lifetime.

In Sec. II we summarize the standard estimate procedures of UCN loss rate in material traps and emphasize their approximations. In Sec. III we analytically calculate the UCN absorption rate for two simple trap shapes and show the difference between various estimate methods of UCN loss-rate calculations. In Sec. IV we discuss their consequences on the size scaling and on the accuracy of estimates of neutron loss rate and lifetime.

II. STANDARD ESTIMATE PROCEDURE OF NEUTRON LOSSES IN UCN TRAPS AND ITS DISCUSSION

A. Basic formulas

The methods of estimating τ_{loss}^{-1} start from the well-known formula [21–23] for the absorption probability of neutron by the wall during each scattering

$$\mu(v_{\perp}) = \frac{2\eta v_{\perp}/v_{\text{lim}}}{\sqrt{1 - (v_{\perp}/v_{\text{lim}})^2}}, \quad (1)$$

where η is the loss coefficient depending on the wall material, v_{\perp} is the normal-to-wall UCN velocity, and to the v_{lim} is the limiting velocity, corresponding to the UCN kinetic energy E_k equal to the potential barrier $V_0 = m_n v_{\text{lim}}^2/2$, created by trap material. Then one usually assumes a uniform distribution of the incidence angle of UCN on the walls. The integration of Eq. (1) over the solid incidence angle gives another well-known formula [21–23] for the averaged absorption probability

$$\bar{\mu}(v_*) = \frac{2\eta}{v_*^2} \left(\arcsin v_* - v_* \sqrt{1 - v_*^2} \right) \approx \begin{cases} \pi\eta, & v_* \rightarrow 1 \\ 4\eta v_*/3, & v_* \ll 1 \end{cases}, \quad (2)$$

where the normalized velocity $v_* \equiv v/v_{\text{lim}} = \sqrt{E_k/V_0}$. We rewrite Eq. (2) as

$$\bar{\mu}(E_*) = 2\eta f_1(E_*), \quad (3)$$

introducing the normalized UCN energy $E_* \equiv E_k/V_0 = v_*^2$ and the dimensionless function

$$f_1(x) = \frac{1}{x} \left(\arcsin \sqrt{x} - \sqrt{x} \sqrt{1-x} \right), \quad (4)$$

which describes the effective collision rate of UCN with trap walls.

B. Gravity effects and size extrapolation

The averaged absorption probability $\bar{\mu}$ depends on UCN kinetic energy E_k , which due to the Earth gravity depends on the height h above the trap bottom as $E_k(h) = E - m_n g h = E - h'$, where E is total UCN energy, equal to the kinetic neutron energy at the trap bottom $h = 0$, g is the free-fall acceleration, and $h' \equiv m_n g h$. The corresponding height dependence of neutron velocity $v_*(h) = \sqrt{(E - m_n g h)/V_0}$ is, usually, taken into account by the integration of the averaged scattering rate $\bar{\mu}(E_k)$ over the trap surface as [24, 27]

$$\tau_{(g)}^{-1}(E) = \frac{\int_0^{h_{\text{max}}(E)} dS(h) \bar{\mu}(E - h') v(E - h') \rho(E, h')}{4 \int_0^{h_{\text{max}}(E)} dV(h) \rho(E, h')} \equiv \eta \gamma(E), \quad (5)$$

where according to Ref. [27] the UCN number density

$$\rho(E, h) \propto \sqrt{(E - h')/E} \quad (6)$$

gives the energy and height distribution of UCN in the trap,

$$h_{\text{max}}(E) \equiv E/m_n g = v^2/2g \equiv h_{\text{lim}} E_* \quad (7)$$

is the maximal height of neutrons with energy E , and $\gamma(E)$ is the effective collision frequency of UCN with the walls. This effective UCN collision frequency also enters the size extrapolation formula that gives the neutron β -decay time τ_n from two measured lifetimes τ_1 and τ_2 in two UCN traps of different size [27]:

$$\tau_n^{-1} = \tau_1^{-1} - \left(\tau_2^{-1} - \tau_1^{-1} \right) \left/ \left(\frac{\gamma_2(E)}{\gamma_1(E)} - 1 \right) \right. . \quad (8)$$

For the traps of height $h \ll h_{\text{lim}}$ one can simplify further, ignoring the gravity effects and assuming the isotropic velocity distribution. The ratio of effective collision frequencies is then taken as the ratio of surface-to-volume ratios of two different traps [22]:

$$\frac{\gamma_2(E)}{\gamma_1(E)} = \frac{S_2}{V_2} \bigg/ \frac{S_1}{V_1} . \quad (9)$$

According to Eq. (9), one obtains the following simple formula for the UCN loss rate

$$\tau_{(s)}^{-1}(E) = \frac{\bar{\mu}(E) v(E) S}{4V} . \quad (10)$$

Below we compare these two results, given by Eqs. (5) and (10), with the calculated exact result for several simple trap shapes.

C. Problems with standard size extrapolation and with estimates of UCN losses

Evidently, Eq. (9) is oversimplified and contradicts Eq. (5), because the two UCN traps are, usually, not geometrically similar. Even if they are similar in shape and differ only in size, the gravity effects violate the simple formula (9). Therefore, in Refs. [24, 27] Eq. (5) was used to estimate $\gamma(E)$. However, the energy dependence of $\tau_{(g)}^{-1}(E)$ and $\gamma(E)$ in Eq. (5) makes the size extrapolation to be energy dependent too. This problem can be partially solved by the integration of the result for $\tau_{(g)}^{-1}(E)$ over energy with the actual energy distribution $n(E)$ of UCN. Then the final τ_n result (8) depends on the distribution function $n(E)$. This function is unknown. In Ref. [27] it was initially assumed Maxwellian and then corrected by fitting the energy spectrum of UCN reaching the detector, which can be measured. However, even this fitting procedure does not ensure that the distribution function $n(E)$ is found precisely.

Another important problem is that Eqs. (3) and (5) are also approximate, because the gravity changes not only the neutron energy but also the velocity distribution, because it affects only the vertical z -component of UCN velocity. This has two main effects on the estimate procedure of UCN losses. First, the assumption of uniform angular distribution of UCN velocities, implied in Eqs (3) and (5), holds at the trap bottom but violates on the side trap walls at any $h \neq 0$. Probably, this anisotropy of velocity distribution can be compensated by a proper choice of the function $\bar{\mu}^*(y)$, which now should depend on the trap size and geometry. By the Monte-Carlo simulations it was shown [27] that while the result of energy extrapolation is very sensitive to the function $\bar{\mu}(y)$ and differs by 40 seconds for different $\bar{\mu}(y)$, the result of subsequent size extrapolation is much less sensitive to the function $\bar{\mu}(y)$ and varies within the interval of only 4 seconds. Second, even if the UCN velocity distribution was isotropic, the dependence of collision rate on the vertical UCN velocity strongly differs from that for horizontal, as follows from Eq. (12) below. Hence, the effective collision rate is not given by Eqs. (2)-(4), which affects the accuracy of UCN loss estimates.

There is a more fundamental question about the validity of Eq. (1) for the neutron absorption rate during the collisions, especially for the walls with imperfections as pores or rough unflat surface. This problem can be partially solved covering the trap wall by a liquid film, as ^4He in the proposal of Refs. [53–59]. However, the typical experiments are performed at higher temperature and with solid trap walls, e.g. the Fomblin grease [24–30]. In this paper we assume Eq. (1) to be valid, and for several simple UCN trap shapes we analyze the effect of

the above mentioned anisotropy of UCN velocity distribution and of effective collision frequency on the UCN loss rate and on the accuracy of τ_n extraction.

III. ANALYTICAL FORMULAS FOR UCN LOSS RATE FOR RECTANGULAR AND CYLINDRICAL TRAP SHAPES

For a rectangular UCN trap of size $L_x \times L_y \times L_z$ the neutron motion along three main axes separate, because any elastic scattering by the trap wall perpendicular to axis i only changes the sign of neutron velocity v_i along this axis. The absorption probability during each collision is given by Eq. (1) and also depends only on the same velocity component $v_i = v_{\perp}$:

$$\mu_i(v_i) = \frac{2\eta v_i/v_{\text{lim}}}{\sqrt{1 - v_i^2/v_{\text{lim}}^2}}. \quad (11)$$

The number of collisions with the walls during a long time $t \gg L_i/v_i$ can be easily estimated:

$$N_x = \frac{tv_x}{L_x}, \quad N_y = \frac{tv_y}{L_y}, \quad N_z = \frac{tg}{2v_z}, \quad (12)$$

where the vertical velocity component v_z is taken at the trap bottom $z = 0$. From Eq. (12) we already see a strong difference between the dependence of UCN collision rate on their vertical and horizontal velocities. While the collision rate with side walls is proportional to the horizontal UCN velocity and is not affected free fall acceleration, the collision rate with trap bottom is inversely proportional to the vertical UCN velocity, because there is no upper trap wall, and the neutrons fall to the bottom only because of gravity. Hence, there is a big difference between the collisions with trap bottom and side walls, which affects the usual procedure of size extrapolation of UCN loss rate to an infinitely large UCN trap.

The probability for a neutron to remain in the trap after time t is given by the product

$$P_n(t, \mathbf{v}) = P(t, \mathbf{v})e^{-t/\tau_n}, \quad (13)$$

where the probability for a neutron to be not absorbed by the trap walls is

$$P(t, \mathbf{v}) = \prod_{i=x,y,z} [1 - \mu_i(v_i)]^{N_i}. \quad (14)$$

Since $\mu_i(v_i) \sim \eta \ll 1$ and $N_i \sim \eta^{-1} \gg 1$, using $e = \lim_{n \rightarrow \infty} (1 + 1/n)^n$ one may simplify Eq. (14) to

$$P(t, \mathbf{v}) \approx \exp\left(-\sum_i N_i \mu_i(v_i)\right) = \exp\left(-\frac{t}{\tau_{(e)}(\mathbf{v})}\right), \quad (15)$$

where the exact absorption rate

$$\tau_{(e)}^{-1}(\mathbf{v}) = \sum_i \frac{\mu_i(v_i) N_i}{t}. \quad (16)$$

Before we considered only the specular UCN reflection from the trap walls. However, there is a small probability $P_d \lesssim$

0.1 of a diffuse UCN reflection by an arbitrary angle, which conserves only the absolute value of UCN velocity and its energy. This elastic diffuse reflection is much more probable than the UCN inelastic scattering or absorption, $P_d \gg \eta$, and must be considered. The rare diffuse scatterings mean that the UCN velocity direction in Eq. (15) after many reflections becomes arbitrary. To take this probability P_d into account, we average Eq. (16) over the velocity directions taking their isotropic distribution:

$$\tau_{(e)}^{-1}(E) = \int \frac{d\Omega}{4\pi} \tau_{(e)}^{-1}(\mathbf{v}). \quad (17)$$

As the neutrons reflect specularly many times before their diffusive scattering, Eqs. (15) and (16) remain valid between the diffuse reflections, and the replacement $\tilde{\tau}_{(e)}^{-1}(\mathbf{v}) \rightarrow \tau_{(e)}^{-1}(E)$ accounts for rare diffuse reflections.

Eqs. (16) and (17) should be compared with the generally used formulas for $\tau_{(g)}^{-1}(E)$, given by Eqs. (3)–(6), and with the oversimplified formula for $\tau_{(s)}^{-1}(E)$, given by Eq. (10). The results differ because (i) the probability (15) depends not only on the velocity absolute value as in Eq. (3), but also on its direction, which is not isotropic at finite height h , and (ii) according to Eq. (12) the collision frequency with the trap bottom $N_z \propto v_z^{-1}$ is inversely proportional to the normal velocity, contrary to the collision frequency with the side walls $N_x \propto v_x$ and $N_y \propto v_y$. Below we analytically calculate the UCN absorption rate by the walls of rectangular and cylindrical traps by these three methods and compare the results obtained.

A. Absorption by trap bottom

First, we consider a very wide UCN trap with $L_x, L_y \gg h_{\text{max}}$, where the neutron scattering happens mainly with the trap bottom at $h = 0$. Eqs. (3)–(6), which take the gravity into account but assume (i) an isotropic UCN velocity distribution at any height and (ii) contrary to Eq. (12), the similar dependence of the effective collision rate on the vertical and horizontal UCN velocity, give

$$\tau_{z(g)}^{-1}(E) = \frac{m_n g \bar{\mu}(E) v}{4 \int_0^E dh' \sqrt{1 - h'/E}} = \frac{3}{2} \tau_{z0}^{-1} \frac{f_1(E_*)}{\sqrt{E_*}}. \quad (18)$$

Here we introduced the factor $\tau_{z0}^{-1} = g\eta/v_{\text{lim}}$, which describes the UCN absorption rate by trap bottom in order of magnitude, and the function $f_1(E_*)$ is given by Eq. (4).

When the gravity effects are neglected and an isotropic velocity distribution is assumed, for the size extrapolation in τ_n measurements one often applies Eq. (10) for calculating the UCN loss rate $\tau_{(s)}^{-1}(E)$, which just gives a geometrical surface-to-volume ratio of the UCN trap. This oversimplified method neglecting the gravity seems to be completely inapplicable for the calculation of UCN loss rate due to the collisions with trap bottom, because the corresponding collision rate $N_z = g/2v_z$ in Eq. (12) is determined by gravity. Nevertheless, if we take as the "trap height" V/S in Eqs. (9) and (10) the maximum UCN height in the gravitational potential $h_{\text{max}}(E)$, given by

Eq. (7), then we obtain the following simple formula for the UCN absorption rate

$$\tau_{z(s)}^{-1}(E) = \tau_{z0}^{-1} \frac{f_1(E_*)}{\sqrt{E_*}}. \quad (19)$$

It differs from $\tau_{z(g)}^{-1}(E)$ only by the factor $2/3$, which came from the integral $\int_0^1 dx \sqrt{1-x} = 2/3$ in the denominator of Eq. (18). Physically, this difference comes because Eq. (5) takes into account the dependence of UCN density on height, which is maximal at the trap bottom and, hence, gives a larger absorption rate by the trap bottom, while Eq. (9) assumes a uniform UCN density.

The exact calculation using Eqs. (11), (12), (16) and (17) for an isotropic velocity distribution of UCN near the trap bottom result to a different UCN absorption rate

$$\tau_{z(e)}^{-1}(E) = \tau_{z0}^{-1} \frac{\arcsin \sqrt{E_*}}{\sqrt{E_*}}. \quad (20)$$

Eqs. (18) and (20) give the same value of the UCN absorption rate at $E = 0$ but differ considerably at $E > 0$, which follows already from their Taylor expansions at $E_* = E/V_0 \ll 1$:

$$\frac{\tau_{z(g)}^{-1}}{\tau_{z0}^{-1}} \simeq 1 + \frac{3}{10}E_*, \quad \frac{\tau_{z(e)}^{-1}}{\tau_{z0}^{-1}} \simeq 1 + \frac{E_*}{6}. \quad (21)$$

The oversimplified result in Eq. (19) has both a different UCN absorption rate at $E = 0$ and asymptotics:

$$\frac{\tau_{z(s)}^{-1}}{\tau_{z0}^{-1}} \simeq \frac{2}{3} + \frac{E_*}{5}. \quad (22)$$

The analytical results (18), (19) and (20) are plotted in Fig. 1. They hold for the UCN absorption rate by the trap bottom not only for rectangular but for any straight cylindrical trap with an arbitrary base shape.

B. Absorption by rectangular side walls

Now we consider the UCN absorption by side walls calculated using the above three methods. The standard extrapolation procedure described by Eqs. (3)–(6) for the rectangular trap of dimensions $L_x \times L_y$ gives the following UCN absorption rate by side walls

$$\begin{aligned} \tau_{r(g)}^{-1} &= \frac{L_x + L_y}{2L_x L_y} \frac{\int_0^{h_{\max}(E)} dh \bar{\mu}(E-h') v(E-h') \rho(E, h')}{\int_0^{h_{\max}(E)} dh \rho(E, h')} \\ &= 3\tau_{r0}^{-1} \frac{f_2(E_*)}{\sqrt{E_*}}, \end{aligned} \quad (23)$$

where we introduced the factor $\tau_{r0}^{-1} = \eta v_{\text{lim}}(L_x + L_y)/2L_x L_y$ giving the UCN absorption rate by side trap walls in order of

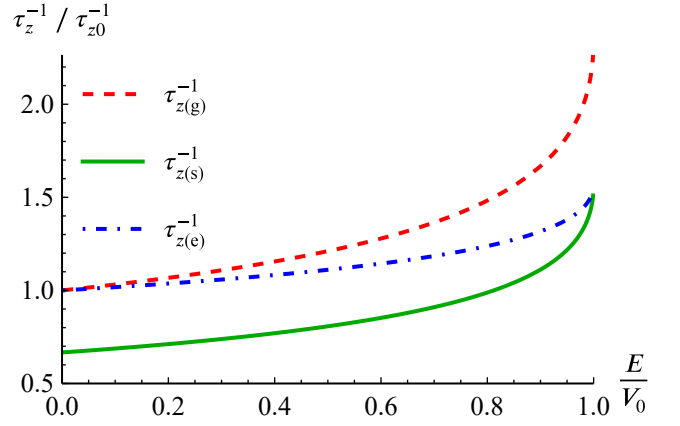


FIG. 1. The energy dependence of UCN loss rate τ_z from the absorption by trap bottom only, corresponding to a wide UCN trap. The calculations and averaging over UCN incidence angle are done in three ways: (i) the standard method, using Eqs. (3)–(6) and resulting to Eq. (18) (dashed red line), which assumes that the gravity only changes the UCN density and velocity absolute value (as a function of height) but not its angular distribution, (ii) the oversimplified method, neglecting all gravity effects and giving Eq. (19) (solid green line), and (iii) the exact calculation method for a wide trap giving Eq. (20) (dot-dashed blue line).

magnitude, and the dimensionless function

$$\begin{aligned} f_2(y) &= \int_0^1 dx \left(\arcsin \sqrt{y(1-x)} - \sqrt{y(1-x)} \sqrt{1-y(1-x)} \right) \\ &= \left(\frac{3}{4y} - \frac{1}{2} \right) \sqrt{y(1-y)} - \left(\frac{3}{4y} - 1 \right) \arcsin \sqrt{y}. \end{aligned} \quad (24)$$

Applying Eq. (10), which neglects gravity, we get the following oversimplified absorption rate by side walls

$$\tau_{r(s)}^{-1}(E) = 2\tau_{r0}^{-1} \sqrt{E_*} f_1(E_*). \quad (25)$$

Combining the exact Eqs. (11),(12),(16),(17) we get the absorption rate by side walls due to the UCN horizontal motion

$$\tau_{r(e)}^{-1} = 2\tau_{r0}^{-1} \sqrt{E_*} f_1(E_*). \quad (26)$$

We see that Eqs. (26) and (25) coincide. This is not surprising because in our model the vertical and horizontal UCN motions along each main axis are separated. For a rectangular UCN trap the absorption rate by side walls depends only on the horizontal UCN velocities, which do not depend on the height h above the trap bottom, as in the oversimplified formula (10). However, as can be seen from Fig. 4 below, a similar coincidence does not hold for arbitrary UCN trap shapes, where the two horizontal UCN velocity components do not separate.

At $E_* \ll 1$ Eqs. (23) and (25) or (26) simplify to

$$\frac{\tau_{r(g)}^{-1}}{\tau_{r0}^{-1}} \simeq \frac{4}{5}E_*, \quad \frac{\tau_{r(s)}^{-1}}{\tau_{r0}^{-1}} = \frac{\tau_{r(e)}^{-1}}{\tau_{r0}^{-1}} \simeq \frac{4}{3}E_*. \quad (27)$$

These low-energy Taylor expansions differ already in the first linear-term coefficient.

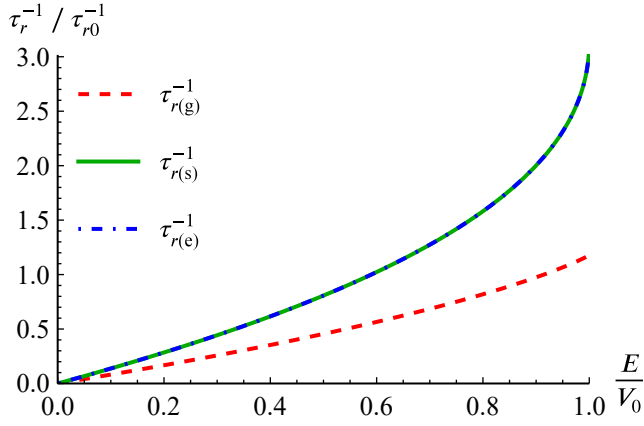


FIG. 2. The energy dependence of UCN loss rate τ_r^{-1} from the absorption by side walls only, corresponding to rectangular $L_x \times L_y$ trap. The calculation is performed in three ways: the standard method, giving Eq. (23) (dashed red), the oversimplified method, giving Eq. (25) (solid green), and the exact calculation method for a rectangular trap, giving Eq. (26) (dot-dashed blue).

In Fig. 2 we compare the UCN absorption rates by side walls given by Eqs.(23),(25) and (26). The result in Eq. (23), obtained by the standard method, differs strongly from that in Eqs. (25) and (26), as one can see already from their Taylor expansions in Eq. (27). This difference appears because Eq. (25), coming from Eqs. (3)–(6), assumes an isotropic UCN velocity distribution at any height. This assumption is not fulfilled because at large height the vertical velocity component is reduced by gravity, while the horizontal UCN velocity is not affected by the gravity. Hence, the normal-to-wall horizontal UCN velocity component, which enters Eq. (1), is larger than the one assumed in Eq. (23). Therefore, Eq. (23) gives a too small absorption rate by side walls. This is especially important for the size extrapolation, which now depends on trap shapes.

C. Absorption by cylindrical side wall

The number of UCN collision with the side wall of a straight vertical cylinder of radius R during a long time $t \gg R/v_{xy}$ and the corresponding absorption rate, in analogy with Eqs. (12) and (16), are given by:

$$\mathcal{N}_c = \frac{t v \sin \theta}{R \text{crd } \varphi}, \quad \tilde{\tau}_{c(e)}^{-1}(v) = \frac{\mu(v_{\perp}) \mathcal{N}_c}{t}, \quad (28)$$

where $\text{crd } \varphi = 2 \sin(\varphi/2)$ is the chord length in a unit circle, and $v \sin \theta$ is the neutron speed in xy plane (see Fig. 3). The neutron velocity component normal to the cylinder walls is expressed as

$$v_{\perp} = v \sin \theta (\tilde{\mathbf{v}}_{xy} \cdot \tilde{\mathbf{n}}_{xy}) = v \sin(\varphi/2) \sin \theta, \quad (29)$$

where $\tilde{\mathbf{v}}_{xy} = (\cos \varphi - 1, \sin \varphi) / \text{crd } \varphi$ is the unit direction vector of UCN velocity in the xy -plane, $\tilde{\mathbf{n}} = (\cos \varphi, \sin \varphi)$ is the unit vector normal to circle in the xy -plane at the intersection point.

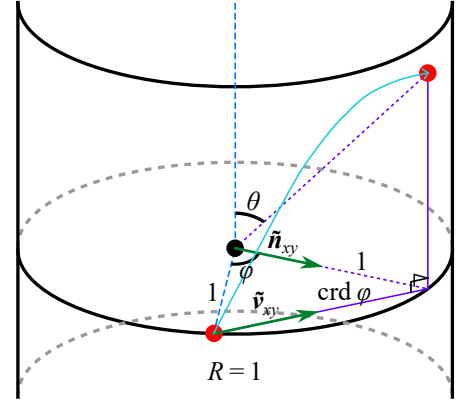


FIG. 3. Neutron path between the reflections from the side wall of a cylindrical trap. This scheme also illustrates the notations, used in the text and formulas.

Averaging Eq. (28) over angles, we get the absorption rate

$$\tau_{c(e)}^{-1} = \tau_{c0}^{-1} \sqrt{E_*} \left(\arcsin \sqrt{E_*} + \frac{f_1(E_*)}{2} \right), \quad (30)$$

where we introduced $\tau_{c0}^{-1} = \eta v_{\text{lim}} / 2R$ describing the UCN absorption rate by cylindrical side wall in the order of magnitude.

The standard calculation method described by Eqs. (3)–(5) for the cylindrical trap of radius R gives the side-wall absorption rate

$$\tau_{c(g)}^{-1}(E) = 3 \tau_{c0}^{-1} \frac{f_2(E_*)}{\sqrt{E_*}}. \quad (31)$$

It resembles the expression (23) derived for the rectangular trap except for the coefficient $\tau_{r0}^{-1} \rightarrow \tau_{c0}^{-1}$.

The oversimplifies method neglecting the gravity and described by Eq. (10) gives

$$\tau_{c(s)}^{-1}(E) = 2 \tau_{c0}^{-1} \sqrt{E_*} f_1(E_*). \quad (32)$$

The results given by Eqs. (32) and (30) differ, which follows from the quadratic term of their Taylor expansions at $E_* \ll 1$:

$$\frac{\tau_{c(s)}^{-1}}{\tau_{c0}^{-1}} \simeq \frac{4}{3} E_* + \frac{2}{5} E_*^2, \quad \frac{\tau_{c(e)}^{-1}}{\tau_{c0}^{-1}} \simeq \frac{4}{3} E_* + \frac{4}{15} E_*^2. \quad (33)$$

Eq. (31), corresponding to the standard calculation method, differs from two other methods much stronger, already in the linear order:

$$\frac{\tau_{c(g)}^{-1}}{\tau_{c0}^{-1}} \simeq \frac{4}{5} E_*. \quad (34)$$

In Fig. 4 we compare the UCN absorption rates by cylindrical side walls calculated by all three methods and given by Eqs. (30),(31) and (32). We see that the results of exact and oversimplified methods, given by Eqs. (30) and (32) correspondingly, now differ but not strongly, mainly at large neutron energy approaching the potential barrier height V_0 .

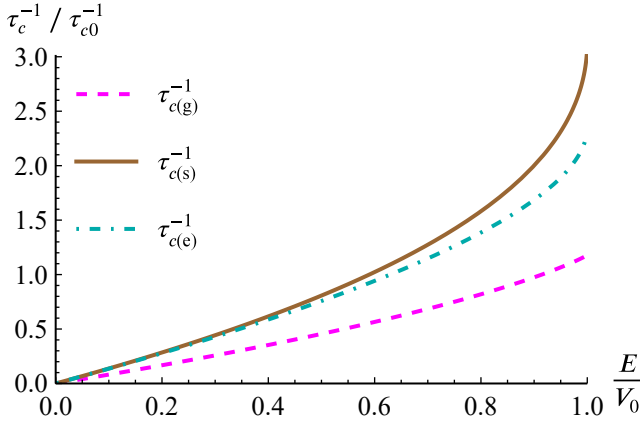


FIG. 4. The energy dependence of UCN loss rate τ_c^{-1} from the absorption by side wall of a straight cylindrical trap of radius R . The calculation and averaging over the UCN incidence angle is performed in three ways: the standard method, giving Eq. (31) and shown by dashed magenta line, the oversimplified method, resulting to Eq. (32) (solid brown line), and the exact calculation method for a cylindrical trap, giving Eq. (30) (dot-dashed cyan line).

On contrary, the UCN loss rates calculated by the standard method and given by Eq. (31) is very different. This difference is similar to the case of rectangular side walls, considered in Sec. III B and illustrated in Fig. 2, and have the same origin, discussed in the end of Sec. III B.

D. Total absorption rate and size extrapolation

From Figs. 1, 2, and 4 we see that the UCN absorption rate and its dependence on UCN energy differ strongly for trap bottom and side walls. This means that the UCN absorption rate changes differently if the trap dimensions are reduced along the vertical z or horizontal x, y axes. This is very important because it affects the procedure of size extrapolation, on which all current precise τ_n UCN storage measurements are based to account for the difference $\geq 2\%$ between the measured and extracted neutron lifetime. Our calculations show that the result of the size extrapolation depends strongly on the shapes of large and reduced UCN traps, i.e. on the position and shape of the trap insert in UCN- τ experiments.

To illustrate this message and to estimate possible error in the estimates of neutron loss rate we now compare the UCN absorption rate calculated using the above three methods for a rectangular (cylindrical) UCN trap of typical dimensions $L_x, L_y \sim h_{\text{lim}}$ for rectangular and $R \sim h_{\text{lim}}$ for cylindrical traps. Evidently, the total absorption rate τ^{-1} is given by the sum of the absorption rate τ_z^{-1} by trap bottom due to the vertical UCN motion and the absorption rate τ_r^{-1} (τ_c^{-1}) by side walls due to the horizontal UCN velocity.

For the rectangular trap the total absorption rate

$$\tau_R^{-1}(E_*) = \tau_z^{-1}(E_*) + \tau_r^{-1}(E_*). \quad (35)$$

It is convenient to introduce the dimensionless parameter $h_* = h_{\text{lim}}(L_x + L_y)/2L_xL_y = h_{\text{lim}}(L_x^{-1} + L_y^{-1})/2$, which describes

the UCN trap size and enters all the expressions for absorption rate. At $L_x = L_y = L$ this size parameter $h_* = h_{\text{lim}}/L$, and $\tau_{r0}^{-1} = 2\tau_{z0}^{-1}h_*$. Combining Eqs. (35), (19) and (25) we obtain for the oversimplified method without gravity the following total UCN absorption rate:

$$\tau_{R(s)}^{-1}(E_*) = \tau_{z0}^{-1} \frac{f_1(E_*)}{\sqrt{E_*}} (1 + 4h_*E_*). \quad (36)$$

Combining Eqs. (35), (18) and (23) gives the result of standard method where the gravity changes only the UCN energy and concentration as a function of height:

$$\tau_{R(g)}^{-1}(E_*) = \frac{3}{2}\tau_{z0}^{-1} \frac{f_1(E_*)}{\sqrt{E_*}} \left(1 + 4h_* \frac{f_2(E_*)}{f_1(E_*)}\right). \quad (37)$$

The exact Eqs. (35), (20) and (26) give the following total UCN absorption rate by the walls of rectangular trap:

$$\tau_{R(e)}^{-1}(E_*) = \tau_{z0}^{-1} \frac{f_1(E_*)}{\sqrt{E_*}} \left(\frac{\arcsin \sqrt{E_*}}{f_1(E_*)} + 4h_*E_*\right). \quad (38)$$

Let us compare a rectangular trap with a cylindrical one at the same volume to height ratio, i.e. the same base area $V/h_{\text{lim}} = L^2 = \pi R^2$. Then $h_* = h_{\text{lim}}/(R\sqrt{\pi})$ and $\tau_{c0}^{-1} = \sqrt{\pi}\tau_{z0}^{-1}h_*$. Performing the same steps as for a rectangular trap, but using

$$\tau_C^{-1}(E_*) = \tau_z^{-1}(E_*) + \tau_c^{-1}(E_*) \quad (39)$$

instead of Eq. (35), we get the analytical formulas for the total UCN absorption rate in a cylindrical trap for all three methods. Combining Eqs. (39), (19) and (32) we obtain the oversimplified result

$$\tau_{C(s)}^{-1}(E_*) = \tau_{z0}^{-1} \frac{f_1(E_*)}{\sqrt{E_*}} (1 + 2\sqrt{\pi}h_*E_*), \quad (40)$$

Combining Eqs. (39), (18) and (31) gives the standard-method estimate of UCN absorption rate

$$\tau_{C(g)}^{-1}(E_*) = \frac{3}{2}\tau_{z0}^{-1} \frac{f_1(E_*)}{\sqrt{E_*}} \left(1 + 2\sqrt{\pi}h_* \frac{f_2(E_*)}{f_1(E_*)}\right), \quad (41)$$

Eqs. (39), (20) and (30) based on exact formulas give

$$\tau_{C(e)}^{-1}(E_*) = \tau_{z0}^{-1} \left[\frac{\arcsin \sqrt{E_*}}{\sqrt{E_*}} (1 + \sqrt{\pi}h_*E) + \frac{\sqrt{\pi}}{2} h_* \sqrt{E_*} f_1(E) \right]. \quad (42)$$

In Fig. 5 we compare the geometrical size scaling of UCN loss rates in a rectangular and cylindrical traps calculated by three different methods for a typical UCN energy $E = V_0/2$. The green and brown solid lines show the oversimplified result in Eqs. (36) and (40) for rectangular and cylindrical traps correspondingly, where the gravity effects are neglected and the isotropic velocity distribution of UCN is assumed. The red

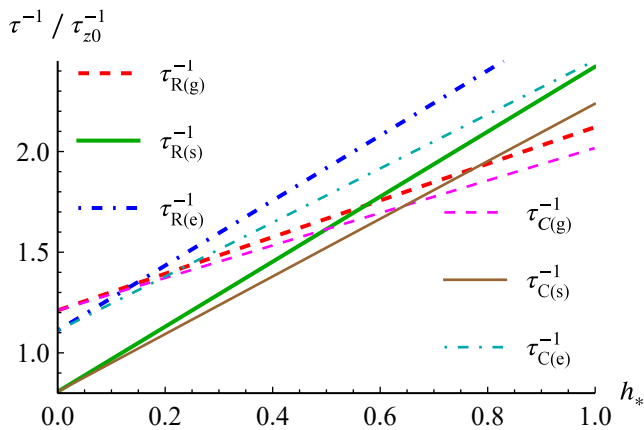


FIG. 5. The dependence of UCN loss rate τ^{-1} on the reduced inverse trap size h_* at $E_* = 1/2$. Rectangular and cylindrical traps are taken with equal areas, so that $L = R\sqrt{\pi}$. The averaging over the UCN incidence angle is performed in three ways: (i) the standard method, resulting to Eqs. (37) and (41) and illustrated by dashed lines (the red line corresponds to rectangular trap and the magenta line corresponds to cylindrical trap), (ii) the oversimplified method, neglecting all gravity effects and giving Eqs. (36) and (40) (green and brown solid lines), and (iii) the exact calculation method resulting to Eqs. (38) and (42), shown by the blue and cyan dot-dashed lines.

and magenta dashed lines illustrate the improved approximate formulas (5) and (3), applied in Refs. [24, 27] and resulting to Eqs. (37) and (41), where the gravity effect is included via the height-dependent UCN energy and concentration, but the isotropic velocity distribution of UCN is assumed at any height and the collision rate with trap bottom is proportional to UCN vertical velocity. The dot-dashed blue and cyan lines show the UCN absorption rates by rectangular and cylindrical trap walls given by Eqs. (38) and (42), calculated exactly for specular UCN reflections and taking into account rare diffuse isotropic scattering events resulting to angular averaging.

As one can see from Fig. 5 or from Eqs. (37)-(42), the absorption rate τ^{-1} depends linearly on h_* . All three calculation methods give very different values $\tau^{-1}(h_* = 0)$, corresponding to the absorption rate by trap bottom only and describing a very wide UCN trap. This difference exceeds 10% even for the improved approximate method including gravity, which may result to the error up to ~ 2 seconds in the estimate of neutron lifetime τ_n . Hence, the size extrapolation by changing the trap base area gives very different UCN absorption rates for the considered three methods.

The linear $\tau^{-1}(h_*)$ dependence and the same value $\tau^{-1}(h_* = 0)$ for the rectangular and cylindrical traps calculated by the same method can be used to scale the plots in Fig. 5 by changing the definition of h_* for the cylindrical trap from $h_* = h_{\text{lim}}/(R\sqrt{\pi})$ to $h_* = h_{\text{lim}}/(2R)$, corresponding to $L = 2R$ and $\tau_{z0}^{-1} = 2\tau_{z0}^{-1}h_*$. In this case, the standard and oversimplified formulas for cylindrical trap coincide exactly with those obtained for a rectangular trap and given by Eqs. (37), (36). This is illustrated in Fig. 6. Only the exact method gives slightly different results for cylindrical and rectangular traps with the deviation less than 4%, see Fig. 6), because it explic-

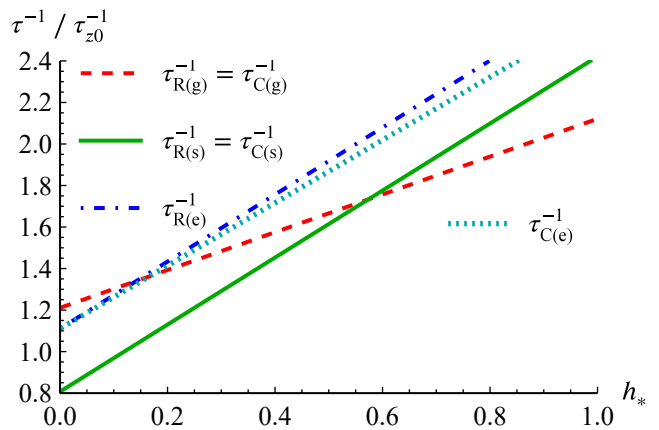


FIG. 6. The dependence of UCN loss rate τ^{-1} on the reduced inverse trap size h_* at $E_* = 1/2$. The difference from Fig. 5 is that here the comparison is at $L = 2R$.

itly takes into account the specular reflection of neutrons from the cylindrical walls:

$$\tau_{C(e)}^{-1}(E_*) = \tau_{z0}^{-1} \left[\frac{\arcsin \sqrt{E_*}}{\sqrt{E_*}} (1 + 2h_*E) + h_*\sqrt{E_*}f_1(E) \right]. \quad (43)$$

IV. DISCUSSION AND CONCLUSIONS

In this paper we reanalyze the standard calculation methods of UCN absorption rate by the walls of material traps, which is crucial for the accuracy of neutron lifetime measurements. The standard analytical formulas (3)–(6) take the gravity into account but assume (i) an isotropic UCN velocity distribution at any height and (ii) the similar dependence of the effective collision rate on the vertical and horizontal UCN velocity. The latter evidently contradicts Eq. (12) giving the exact collision rates for rectangular UCN traps, where the vertical and horizontal neutron motion separate. To analyze how these approximations of the standard method affect the estimates of neutron loss rate we calculate the UCN absorption rate by the rectangular and cylindrical trap walls without these assumptions, i.e. using more fundamental Eqs. (12) and (1).

Fortunately, we succeed to perform these calculations analytically, which allows the simple analysis and comparison of our results for the UCN loss rates calculated by three different methods: (1) the oversimplified method, neglecting gravity at all and based on Eqs. (9) and (10); (2) the improved approximate formulas (3)–(6), applied in Refs. [24, 27] as a standard method, where the gravity effect is included via the height-dependent UCN energy and concentration only; (3) by a direct calculation using the initial equations (1) and (12).

Our results, illustrated in Figs. 1-6, show that (i) the UCN absorption rates calculated by these three methods differ considerably, by $\geq 10\%$ both for rectangular and cylindrical traps, and (ii) the results of size extrapolation depend strongly on the trap shape and, hence, must be done with a great care. The former is evidently important because may give an error up to

few seconds in the extracted neutron lifetime τ_n . The latter is also very important because the size scaling and extrapolation to an infinite trap is a standard and necessary procedure for extracting τ_n . We have shown that the change of trap dimensions along the vertical and horizontal directions affects the UCN loss rate $\bar{\tau}_a^{-1}$ differently. Hence, the results of size extrapolation in UCN- τ experiments depend both on the trap shape and size, as well as on the insert position, size and shape. The approximate formulas (3)–(6) do not describe this dependence accurately enough.

The obtained large difference $\geq 10\%$ between the UCN absorption rate estimated by the standard method based on Eqs. (3)–(6) and calculated using the exact Eqs. (1) and (12) is a consequence of effective separation between the vertical and horizontal neutron motion for the chosen trap shapes in the form of straight vertical cylinders with a rectangular or circle base. For these trap shapes the very different dependence of the UCN collision rate on their vertical and horizontal velocity components, given by Eq. (12) and disregarded by Eqs. (3)–(6), results to the obtained large difference of various calculation methods. In our model and for the chosen trap shapes the vertical and horizontal neutron motion are coupled only due to the rare diffuse scattering. Hence, the separation of vertical and horizontal UCN motion, conserved by the usual specular reflections, holds during a long time between rare diffuse scattering events and affects the UCN absorption during multiple scattering by trap walls. In the experiment of Ref. [27] the UCN trap and insert were the horizontal half cylinders of different radii. For such horizontal rather than vertical cylinder traps the considered separation of vertical and horizontal UCN motion does not hold even during the specular reflections by trap walls. Hence, for these trap and insert shapes the difference between the UCN absorption rates calculated by different methods is expected to be much smaller than in our model. Nevertheless, it may still considerably affect the size extrapolation and be important for the precise neutron lifetime measurements.

A possible way to increase the accuracy of UCN loss-rate estimates is to use the Monte-Carlo simulations [46–51], where the trajectory of each neutron is calculated with allowance for gravity. With some accuracy, these simulations confirm [27, 46, 47, 49, 50] the results based on approximate formulas (3)–(6) and used to analyze the experimental data in Refs. [24, 27]. However, the physical model used in these numerical calculations requires some clarification. In the Monte-Carlo simulations, usually, the Lambert’s cosine law of the angu-

lar dependence of UCN diffuse scattering intensity is applied [46–51]. Even in optics this Lambert’s cosine law is not universal and there are many deviations from it [62–64], which are quite important in the optical spectroscopy, e.g., used for biological analysis [64]. For the diffuse neutron scattering there is no strict derivation of the Lambert’s cosine law at all. The short-range defects in the trap walls, having the characteristic size smaller than the UCN wave length $\lambda \sim 100$ nm, give the uniform angular distribution of diffusive UCN scattering probability rather than the Lambert’s cosine law. These short-range wall imperfections include the surface roughness, nanopores, impurities, etc. Therefore in our analysis we used the isotropic velocity distribution after the rare diffuse scattering. The long-range wall roughness or large pores of size $d \gg \lambda$ in the trap material, which scatter with a small wavevector transfer $\sim 1/d$, smear the specular reflection peak in the angular distribution of UCN velocity after the diffuse scattering but do not give the Lambert’s cosine law either. The angular distribution of UCN velocity after the diffuse scattering by a real trap wall is an interesting fundamental problem, which is beyond the scope of this paper. However, the estimates of UCN loss probability and the corresponding accuracy of τ_n -measurements depend strongly on this issue.

To summarize, we discuss the approximations and possible errors of the standard calculations of neutron loss rate due to the absorption by trap walls, which are very important for the precise measurements of neutron lifetime and, possibly, of its electric dipole moment. To illustrate the effect of these approximations we calculate the neutron absorption rate by the walls of rectangular and cylindrical UCN traps using three different methods. Our results show that the standard calculation method of UCN absorption rate may give a considerable error, especially during the size extrapolation used to extract the neutron lifetime from experimental data. This may partially explain a four-second discrepancy between the results of recent precise neutron lifetime measurements in magnetic [36] and material [27] UCN traps. The Monte-Carlo simulations may help to solve this problem, but a physical model of diffuse neutron scattering by trap walls must be elaborated to raise the precision and reliability of these simulations.

V. ACKNOWLEDGMENTS

The work of V.D.K. and P.D.G. is supported by the Russian Science Foundation grant # 23-22-00312.

-
- [1] D. Dubbers and M. G. Schmidt, *Rev. Mod. Phys.* **83**, 1111 (2011), <https://link.aps.org/doi/10.1103/RevModPhys.83.1111>.
- [2] H. Abele, *Progress in Particle and Nuclear Physics* **60**, 1 (2008), <https://www.sciencedirect.com/science/article/pii/S0146641007000622>.
- [3] M. Gonzalez-Alonso, O. Naviliat-Cuncic, and N. Severijns, *Progress in Particle and Nuclear Physics* **104**, 165 (2019), <https://www.sciencedirect.com/science/>

- [article/pii/S0146641018300735](https://www.sciencedirect.com/science/article/pii/S0146641018300735).
- [4] M. Gorchtein and C.-Y. Seng, *Universe* **9**, 422 (2023).
- [5] M. J. Ramsey-Musolf and S. Su, *Physics Reports* **456**, 1 (2008), <https://www.sciencedirect.com/science/article/pii/S0370157307003894>.
- [6] F. E. Wietfeldt and G. L. Greene, *Rev. Mod. Phys.* **83**, 1173 (2011), <https://link.aps.org/doi/10.1103/RevModPhys.83.1173>.

- [7] H. Abele, A. Alekou, A. Algora, K. Andersen, S. Baessler, L. Barron-Palos, J. Barrow, E. Baussan, P. Bentley, Z. Berezhi-ani, Y. Bessler, A. Bhattacharyya, A. Bianchi, J. Bijness, C. Blanco, N. B. Kraljevic, M. Blennow, K. Bodek, M. Bogomilov, C. Bohm, B. Bolling, E. Bouquerel, G. Brooijmans, L. Broussard, O. Buchan, A. Burgman, H. Calen, C. Carlile, J. Cederkall, E. Chanel, P. Christiansen, V. Cirigliano, J. Collar, M. Collins, C. Crawford, E. C. Morales, P. Cupial, L. D'Alessi, J. M. Damian, H. Danared, D. Dancila, J. de Andre, J. De- lahaye, S. Degenkolb, D. Di Julio, M. Dracos, K. Dunne, I. Efthymiopoulos, T. Ekelöf, L. Eklund, M. Eshraqi, I. Es- teban, G. Fanourakis, A. Farricker, E. Fernandez-Martinez, M. Ferreira, M. Fertl, P. Fierlinger, B. Folsom, A. Frank, A. Fratangelo, U. Friman-Gayer, T. Fukuda, H. Fynbo, A. G. Sosa, N. Gazis, B. Galnander, T. Geralis, M. Ghosh, G. Gokbulut, J. Gomez-Cadenas, M. Gonzalez-Alonso, F. Gonzalez, L. Halic, C. Happe, P. Heil, A. Heinz, H. Herde, M. Holl, T. Jenke, M. Jenssen, E. Jericha, H. Johansson, R. Johans- son, T. Johansson, Y. Kamyshkov, A. K. Topaksu, B. Kildetoft, K. Kirch, B. Kliček, E. Klinkby, R. Kolevatov, G. Konrad, M. Koziol, K. Krhac, A. Kupsc, L. Lacny, L. Larizgoitia, C. Lewis, M. Lindroos, E. Lychagin, E. Lytken, C. Maiano, P. Marciniowski, G. Markaj, B. Markisch, C. Marrelli, C. Mar- tins, B. Meirose, M. Mezzetto, N. Milas, D. Milstead, F. Monra- bal, G. Muhrer, A. Nepomuceno, V. Nesvizhevsky, T. Nils- son, P. Novella, M. Oglakci, T. Ohlsson, M. Olvegard, A. Os- karsson, T. Ota, J. Park, D. Patrzalek, H. Perrey, M. Persoz, G. Petkov, F. Piegsa, C. Pistillo, P. Poussot, P. Privitera, B. Rataj, D. Ries, N. Rizzi, S. Rosauero-Alcaraz, D. Rozpedzik, D. Saiang, V. Santoro, U. Schmidt, H. Schober, I. Schulthess, S. Silver- stein, A. Simon, H. Sina, J. Snamina, W. Snow, T. Soldner, G. Stavropoulos, M. Stipcevic, B. Szybinski, A. Takibayev, Z. Tang, R. Tarkeshian, C. Theroine, J. Thorne, F. Terran- ova, J. Thomas, T. Tolba, P. Torres-Sanchez, E. Trachanas, R. Tsenov, U. Uggerhoj, G. Vankova-Kirilova, N. Vassilopou- los, R. Wagner, X. Wang, E. Wildner, M. Wolke, J. Wurtz, S. Yiu, S. Yoon, A. Young, L. Zanini, J. Zejma, D. Zerzion, O. Zimmer, O. Zormpa, and Y. Zou, *Physics Reports* **1023**, 1 (2023), particle Physics at the European Spallation Source.
- [8] G. J. Mathews, T. Kajino, and T. Shima, *Phys. Rev. D* **71**, 021302 (2005).
- [9] B. Märkisch, H. Mest, H. Saul, X. Wang, H. Abele, D. Dubbers, M. Klopff, A. Petoukhov, C. Roick, T. Soldner, and D. Werder, *Phys. Rev. Lett.* **122**, 242501 (2019), <https://link.aps.org/doi/10.1103/PhysRevLett.122.242501>.
- [10] M. Beck, W. Heil, C. Schmidt, S. Baeßler, F. Glück, G. Konrad, and U. Schmidt, *Phys. Rev. Lett.* **132**, 102501 (2024).
- [11] J. Liu, M. P. Mendenhall, A. T. Holley, H. O. Back, T. J. Bowles, L. J. Broussard, R. Carr, S. Clayton, S. Currie, B. W. Filip- pone, A. García, P. Geltenbort, K. P. Hickerson, J. Hoagland, G. E. Hogan, B. Hona, T. M. Ito, C.-Y. Liu, M. Makela, R. R. Mammei, J. W. Martin, D. Melconian, C. L. Morris, R. W. Pattie, A. Pérez Galván, M. L. Pitt, B. Plaster, J. C. Ram- sey, R. Rios, R. Russell, A. Saunders, S. J. Seestrom, W. E. Sondheim, E. Tatar, R. B. Vogelaar, B. VornDick, C. Wrede, H. Yan, and A. R. Young (UCNA Collaboration), *Phys. Rev. Lett.* **105**, 181803 (2010), <https://link.aps.org/doi/10.1103/PhysRevLett.105.181803>.
- [12] X. Sun, E. Adamek, B. Allgeier, Y. Bagdasarova, D. B. Berguno, M. Blatnik, T. J. Bowles, L. J. Broussard, M. A.-P. Brown, R. Carr, S. Clayton, C. Cude-Woods, S. Currie, E. B. Dees, X. Ding, B. W. Filippone, A. García, P. Geltenbort, S. Hasan, K. P. Hickerson, J. Hoagland, R. Hong, A. T. Holley, T. M. Ito, A. Knecht, C.-Y. Liu, J. Liu, M. Makela, R. Mammei, J. W. Martin, D. Melconian, M. P. Mendenhall, S. D. Moore, C. L. Morris, S. Nepal, N. Nouri, R. W. Pattie, A. Pérez Galván, D. G. Phillips, R. Picker, M. L. Pitt, B. Plaster, D. J. Salvat, A. Saunders, E. I. Sharapov, S. Sjue, S. Slutsky, W. Sondheim, C. Swank, E. Tatar, R. B. Vogelaar, B. VornDick, Z. Wang, W. Wei, J. W. Wexler, T. Womack, C. Wrede, A. R. Young, and B. A. Zeck (UCNA Collaboration), *Phys. Rev. C* **101**, 035503 (2020), <https://link.aps.org/doi/10.1103/PhysRevC.101.035503>.
- [13] A. N. Ivanov, M. Pitschmann, and N. I. Troitskaya, *Phys. Rev. D* **88**, 073002 (2013).
- [14] C. Abel, S. Afach, N. J. Ayres, C. A. Baker, G. Ban, G. Bi- son, K. Bodek, V. Bondar, M. Burghoff, E. Chanel, Z. Chowd- huri, P.-J. Chiu, B. Clement, C. B. Crawford, M. Daum, S. Emmenegger, L. Ferraris-Bouchez, M. Fertl, P. Flaux, B. Franke, A. Fratangelo, P. Geltenbort, K. Green, W. C. Grif- fith, M. van der Grinten, Z. D. Grujić, P. G. Harris, L. Hayen, W. Heil, R. Henneck, V. H elaine, N. Hild, Z. Hodge, M. Hor- ras, P. Iaydjiev, S. N. Ivanov, M. Kasprzak, Y. Kermaidic, K. Kirch, A. Knecht, P. Knowles, H.-C. Koch, P. A. Koss, S. Komposch, A. Kozela, A. Kraft, J. Krempel, M. Kuźniak, B. Lauss, T. Lefort, Y. Lemi ere, A. Leredde, P. Mohan- murthy, A. Mtchedlishvili, M. Musgrave, O. Naviliat-Cuncic, D. Pais, F. M. Piegsa, E. Pierre, G. Pignol, C. Plonka-Spehr, P. N. Prashanth, G. Qu em ener, M. Rawlik, D. Rebreyend, I. Rien acker, D. Ries, S. Roccia, G. Rogel, D. Rozpedzik, A. Schnabel, P. Schmidt-Wellenburg, N. Severijns, D. Shiers, R. Tavakoli Dinani, J. A. Thorne, R. Virost, J. Voigt, A. Weis, E. Wursten, G. Wyzynski, J. Zejma, J. Zenner, and G. Zsig- mond, *Phys. Rev. Lett.* **124**, 081803 (2020).
- [15] M. Pospelov and A. Ritz, *Annals of Physics* **318**, 119 (2005), <https://www.sciencedirect.com/science/article/pii/S0003491605000539>.
- [16] C. A. Baker, D. D. Doyle, P. Geltenbort, K. Green, M. G. D. van der Grinten, P. G. Harris, P. Iaydjiev, S. N. Ivanov, D. J. R. May, J. M. Pendlebury, J. D. Richardson, D. Shiers, and K. F. Smith, *Phys. Rev. Lett.* **97**, 131801 (2006), <https://link.aps.org/doi/10.1103/PhysRevLett.97.131801>.
- [17] A. P. Serebrov, E. A. Kolomenskiy, A. N. Pirozhkov, I. A. Krasnoschekova, A. V. Vassiljev, A. O. Polushkin, M. S. Lasakov, A. K. Fomin, I. V. Shoka, V. A. Solovey, O. M. Zherebtsov, P. Geltenbort, S. N. Ivanov, O. Zim- mer, E. B. Alexandrov, S. P. Dmitriev, and N. A. Dova- tor, *JETP Letters* **99**, 4 (2014), <https://doi.org/10.1134/S0021364014010111>.
- [18] V. V. Nesvizhevsky, H. G. B orner, A. K. Petukhov, H. Abele, S. Baeßler, F. J. Rueß, T. St oferle, A. Westphal, A. M. Gagarski, G. A. Petrov, and A. V. Strelkov, *Nature* **415**, 297 (2002), <https://doi.org/10.1038/415297a>.
- [19] T. Jenke, G. Cronenberg, J. Burgd orfer, L. A. Chizhova, P. Geltenbort, A. N. Ivanov, T. Lauer, T. Lins, S. Rot- ter, H. Saul, U. Schmidt, and H. Abele, *Phys. Rev. Lett.* **112**, 151105 (2014), <https://link.aps.org/doi/10.1103/PhysRevLett.112.151105>.
- [20] T. Jenke, P. Geltenbort, H. Lemmel, and H. Abele, *Nature Physics* **7**, 468 (2011).
- [21] R. Golub, D. Richardson, and L. S. K., *Ultra-Cold Neutrons* (CRC Press, 1991) <https://doi.org/10.1201/9780203734803>.
- [22] V. K. Ignatovich, *The Physics of Ultracold Neutrons* (Clarendon Press, 1990) <https://isbnsearch.org/isbn/0198510152>.
- [23] V. K. Ignatovich, *Physics-Uspekhi* **39**, 283 (1996), <https://doi.org/10.1070/pu1996v039n03abeh000138>.

- [24] A. P. Serebrov, V. E. Varlamov, A. G. Kharitonov, A. K. Fomin, Y. N. Pokotilovski, P. Geltenbort, I. A. Krasnoschekova, M. S. Lasakov, R. R. Taldaev, A. V. Vassiljev, and O. M. Zhrebtsov, *Phys. Rev. C* **78**, 035505 (2008), <https://link.aps.org/doi/10.1103/PhysRevC.78.035505>.
- [25] S. Arzumanov, L. Bondarenko, S. Chernyavsky, P. Geltenbort, V. Morozov, V. V. Nesvizhevsky, Y. Panin, and A. Strepetov, *Physics Letters B* **745**, 79 (2015), <https://www.sciencedirect.com/science/article/pii/S0370269315002646>.
- [26] A. P. Serebrov, E. A. Kolomenskiy, A. K. Fomin, I. A. Krasnoschekova, A. V. Vassiljev, D. M. Prudnikov, I. V. Shoka, A. V. Chechkin, M. E. Chaikovskii, V. E. Varlamov, S. N. Ivanov, A. N. Pirozhkov, P. Geltenbort, O. Zimmer, T. Jenke, M. Van der Grinten, and M. Tucker, *JETP Letters* **106**, 623 (2017), <https://doi.org/10.1134/S0021364017220143>.
- [27] A. P. Serebrov, E. A. Kolomenskiy, A. K. Fomin, I. A. Krasnoschekova, A. V. Vassiljev, D. M. Prudnikov, I. V. Shoka, A. V. Chechkin, M. E. Chaikovskii, V. E. Varlamov, S. N. Ivanov, A. N. Pirozhkov, P. Geltenbort, O. Zimmer, T. Jenke, M. Van der Grinten, and M. Tucker, *Phys. Rev. C* **97**, 055503 (2018), <https://link.aps.org/doi/10.1103/PhysRevC.97.055503>.
- [28] Pattie, R. W., Callahan, N. B., Cude-Woods, C., Adamek, E. R., Adams, M., Barlow, D., Blatnik, M., D., Bowman, Broussard, L. J., Clayton, S., Currie, S., Dees, E. B., Ding, X., Fellers, D., Fox, W., Fries, E., Gonzalez, F., Geltenbort, P., Hickerson, K. P., Hoffbauer, M. A., Hoffman, K., Holley, A. T., Howard, D., Ito, T. M., Komives, A., Liu, C. Y., M., Makela, Medina, J., Morley, D., Morris, C. L., O'Connor, T., Penttilä, S.I., Ramsey, J.C., Roberts, A., Salvat, D., Saunders, A., Seestrom, S.J., Sharapov, E.I., Sjue, S.K.L., Snow, W.M., Sprow, A., Vanderwerp, J., Vogelaar, B., P.L., Walstrom, Wang, Z., Weaver, H., Wexler, J., Womack, T.L., Young, A.R., and Zeck, B.A., *EPJ Web Conf.* **219**, 03004 (2019), <https://doi.org/10.1051/epjconf/201921903004>.
- [29] W. Mampe, P. Ageron, C. Bates, J. M. Pendlebury, and A. Steyerl, *Phys. Rev. Lett.* **63**, 593 (1989), <https://link.aps.org/doi/10.1103/PhysRevLett.63.593>.
- [30] A. Pichlmaier, V. Varlamov, K. Schreckenbach, and P. Geltenbort, *Physics Letters B* **693**, 221 (2010), <https://www.sciencedirect.com/science/article/pii/S0370269310009792>.
- [31] P. R. Huffman, C. R. Brome, J. S. Butterworth, K. J. Coakley, M. S. Dewey, S. N. Dzhosyuk, R. Golub, G. L. Greene, K. Habicht, S. K. Lamoreaux, C. E. H. Mattoni, D. N. McKinsey, F. E. Wietfeldt, and J. M. Doyle, *Nature* **403**, 62 (2000), <https://doi.org/10.1038/47444>.
- [32] K. K. H. Leung, P. Geltenbort, S. Ivanov, F. Rosenau, and O. Zimmer, *Phys. Rev. C* **94**, 045502 (2016), <https://link.aps.org/doi/10.1103/PhysRevC.94.045502>.
- [33] A. Steyerl, K. K. H. Leung, C. Kaufman, G. Müller, and S. S. Malik, *Phys. Rev. C* **95**, 035502 (2017), <https://link.aps.org/doi/10.1103/PhysRevC.95.035502>.
- [34] V. F. Ezhov, A. Z. Andreev, G. Ban, B. A. Bazarov, P. Geltenbort, A. G. Glushkov, V. A. Knyazkov, N. A. Kovrizhnykh, G. B. Krygin, O. Naviliat-Cuncic, and V. L. Ryabov, *JETP Letters* **107**, 671 (2018), <https://doi.org/10.1134/S0021364018110024>.
- [35] R. W. Pattie, N. B. Callahan, C. Cude-Woods, E. R. Adamek, L. J. Broussard, S. M. Clayton, S. A. Currie, E. B. Dees, X. Ding, E. M. Engel, D. E. Fellers, W. Fox, P. Geltenbort, K. P. Hickerson, M. A. Hoffbauer, A. T. Holley, A. Komives, C.-Y. Liu, S. W. T. MacDonald, M. Makela, C. L. Morris, J. D. Ortiz, J. Ramsey, D. J. Salvat, A. Saunders, S. J. Seestrom, E. I. Sharapov, S. K. Sjue, Z. Tang, J. Vanderwerp, B. Vogelaar, P. L. Walstrom, Z. Wang, W. Wei, H. L. Weaver, J. W. Wexler, T. L. Womack, A. R. Young, and B. A. Zeck, *Science* **360**, 627 (2018), <https://science.sciencemag.org/content/360/6389/627>, <https://science.sciencemag.org/content/360/6389/627.full.pdf>.
- [36] F. M. Gonzalez, E. M. Fries, C. Cude-Woods, T. Bailey, M. Blatnik, L. J. Broussard, N. B. Callahan, J. H. Choi, S. M. Clayton, S. A. Currie, M. Dawid, E. B. Dees, B. W. Filippone, W. Fox, P. Geltenbort, E. George, L. Hayen, K. P. Hickerson, M. A. Hoffbauer, K. Hoffman, A. T. Holley, T. M. Ito, A. Komives, C.-Y. Liu, M. Makela, C. L. Morris, R. Musedinovic, C. O'Shaughnessy, R. W. Pattie, J. Ramsey, D. J. Salvat, A. Saunders, E. I. Sharapov, S. Slutsky, V. Su, X. Sun, C. Swank, Z. Tang, W. Urich, J. Vanderwerp, P. Walstrom, Z. Wang, W. Wei, and A. R. Young (UCN τ Collaboration), *Phys. Rev. Lett.* **127**, 162501 (2021).
- [37] J. S. Nico, M. S. Dewey, D. M. Gilliam, F. E. Wietfeldt, X. Fei, W. M. Snow, G. L. Greene, J. Pauwels, R. Eykens, A. Lamberty, J. V. Gestel, and R. D. Scott, *Phys. Rev. C* **71**, 055502 (2005), <https://link.aps.org/doi/10.1103/PhysRevC.71.055502>.
- [38] A. T. Yue, M. S. Dewey, D. M. Gilliam, G. L. Greene, A. B. Laptev, J. S. Nico, W. M. Snow, and F. E. Wietfeldt, *Phys. Rev. Lett.* **111**, 222501 (2013), <https://link.aps.org/doi/10.1103/PhysRevLett.111.222501>.
- [39] K. Hirota, G. Ichikawa, S. Ieki, T. Ino, Y. Iwashita, M. Kitaguchi, R. Kitahara, J. Koga, K. Mishima, T. Mogi, K. Morikawa, A. Morishita, N. Nagakura, H. Oide, H. Okabe, H. Otono, Y. Seki, D. Sekiba, T. Shima, H. M. Shimizu, N. Sumi, H. Sumino, T. Tomita, H. Uehara, T. Yamada, S. Yamashita, K. Yano, M. Yokohashi, and T. Yoshioka, *Progress of Theoretical and Experimental Physics* **2020**, 10.1093/ptep/ptaa169 (2020), <https://doi.org/10.1093/ptep/ptaa169>, <https://academic.oup.com/ptep/article-pdf/2020/12/123C02/35931162/ptaa169.pdf>.
- [40] S. Rajendran and H. Ramani, *Phys. Rev. D* **103**, 035014 (2021), <https://link.aps.org/doi/10.1103/PhysRevD.103.035014>.
- [41] A. P. Serebrov, M. E. Chaikovskii, G. N. Klyushnikov, O. M. Zhrebtsov, and A. V. Chechkin, *Phys. Rev. D* **103**, 074010 (2021), <https://link.aps.org/doi/10.1103/PhysRevD.103.074010>.
- [42] A. P. Serebrov, *Physics-Uspexhi* **62**, 596 (2019).
- [43] B. Koch and F. Hummel, An exciting hint towards the solution of the neutron lifetime puzzle? (2024), arXiv:2403.00914 [hep-ph].
- [44] D. Dubbers, H. Saul, B. Märkisch, T. Soldner, and H. Abele, *Physics Letters B* **791**, 6 (2019).
- [45] E. A. Goremychkin and Y. N. Pokotilovski, *JETP Letters* **105**, 548 (2017).
- [46] A. K. Fomin and A. P. Serebrov, *Technical Physics* **68**, S424 (2023).
- [47] Fomin, Alexey and Serebrov, Anatolii, *EPJ Web Conf.* **219**, 03001 (2019).
- [48] N. J. Ayres, E. Chanel, B. Clement, P. G. Harris, R. Picker, G. Pignol, W. Schreyer, and G. Zsigmond, Monte carlo simulations for the optimization and data analysis of experiments with ultracold neutrons, in *Proceedings of the International Conference on Neutron Optics (NOP2017)*, Vol. 22 (2018) p. 011032, <https://journals.jps.jp/doi/pdf/10.7566/JPSCP.22.011032>.
- [49] A. K. Fomin and A. P. Serebrov, *Mathematical Models and Computer Simulations* **10**, 741 (2018).
- [50] A. K. Fomin and A. P. Serebrov, *Technical Physics* **62**, 1903 (2017).

- [51] A. P. Serebrov, A. K. Fomin, A. G. Kharitonov, V. E. Varlamov, and A. V. Chechkin, *Technical Physics* **58**, 1681 (2013).
- [52] N. Callahan, C.-Y. Liu, F. Gonzalez, E. Adamek, J. D. Bowman, L. Broussard, S. M. Clayton, S. Currie, C. Cude-Woods, E. B. Dees, X. Ding, W. Fox, P. Geltenbort, K. P. Hickerson, M. A. Hoffbauer, A. T. Holley, A. Komives, S. W. T. MacDonald, M. Makela, C. L. Morris, J. D. Ortiz, R. W. Pattie, J. Ramsey, D. J. Salvat, A. Saunders, E. I. Sharapov, S. K. L. Sjue, Z. Tang, J. Vanderwerp, B. Vogelaar, P. L. Walstrom, Z. Wang, H. Weaver, W. Wei, J. Wexler, and A. R. Young, *Phys. Rev. C* **100**, 015501 (2019).
- [53] R. Golub, C. Jewell, P. Ageron, W. Mampe, B. Heckel, and I. Kilvington, *Zeitschrift für Physik B Condensed Matter* **51**, 187 (1983).
- [54] R. C. Bokun, *Sov. J. Nucl. Phys.* **40**, 287 (1984), <https://inis.iaea.org/search/searchsinglerecord.aspx?recordsFor=SingleRecord&RN=16073419>.
- [55] V. P. Alfimenkov, V. K. Ignatovich, L. P. Mezhov-Deglin, V. I. Morozov, A. V. Strelkov, and T. M. I., *Communications of Joint Institute for Nuclear Research, Dubna preprint (in Russian)* **P3-2009-197** (2009), [http://www1.jinr.ru/Preprints/2009/197\(P3-2009-197\).pdf](http://www1.jinr.ru/Preprints/2009/197(P3-2009-197).pdf).
- [56] P. D. Grigoriev, O. Zimmer, A. D. Grigoriev, and T. Ziman, *Phys. Rev. C* **94**, 025504 (2016), <https://link.aps.org/doi/10.1103/PhysRevC.94.025504>.
- [57] P. D. Grigoriev and A. M. Dyugaev, *Phys. Rev. C* **104**, 055501 (2021).
- [58] P. D. Grigoriev, A. M. Dyugaev, T. I. Mogilyuk, and A. D. Grigoriev, *JETP Letters* **114**, 493 (2021).
- [59] P. D. Grigoriev, A. V. Sadovnikov, V. D. Kochev, and A. M. Dyugaev, *Phys. Rev. C* **108**, 025501 (2023).
- [60] S. Ahmed, E. Altieri, T. Andalib, B. Bell, C. P. Bidinosti, E. Cudmore, M. Das, C. A. Davis, B. Franke, M. Gericke, P. Giampa, P. Gnyp, S. Hansen-Romu, K. Hatanaka, T. Hayamizu, B. Jamieson, D. Jones, S. Kawasaki, T. Kikawa, M. Kitaguchi, W. Klassen, A. Konaka, E. Korkmaz, F. Kuchler, M. Lang, L. Lee, T. Lindner, K. W. Madison, Y. Makida, J. Mammei, R. Mammei, J. W. Martin, R. Matsumiya, E. Miller, K. Mishima, T. Momose, T. Okamura, S. Page, R. Picker, E. Pierre, W. D. Ramsay, L. Rebenitsch, F. Rehm, W. Schreyer, H. M. Shimizu, S. Sidhu, A. Sikora, J. Smith, I. Tanihata, B. Thorsteinson, S. Vanbergen, W. T. H. van Oers, and Y. X. Watanabe (TUCAN Collaboration), *Phys. Rev. C* **99**, 025503 (2019), <https://link.aps.org/doi/10.1103/PhysRevC.99.025503>.
- [61] O. Zimmer, *Phys. Rev. C* **93**, 035503 (2016), <https://link.aps.org/doi/10.1103/PhysRevC.93.035503>.
- [62] T. G. Mayerhöfer, S. Pahlow, and J. Popp, *ChemPhysChem* **21**, 2029 (2020), <https://chemistry-europe.onlinelibrary.wiley.com/doi/pdf/10.1002/cphc.202000464>.
- [63] H. G. Hecht, *J Res Natl Bur Stand A Phys Chem* **80A**, 567 (1976).
- [64] M. Mamouei, K. Budidha, N. Baishya, M. Qassem, and P. A. Kyriacou, *Scientific Reports* **11**, 13734 (2021).